AD-A105 161 ROCKWELL INTERNATIONAL THOUSAND OAKS CA ELECTRONICS--ETC F/G 9/5
PIEZOELECTRIC ZNS FILM ON SILICON.(U)
JUN 81 E J STAPLES F49620-79-C-0022
UNCLASSIFIED ERC41018.3FR AFOSR-TR-81-0682 NL

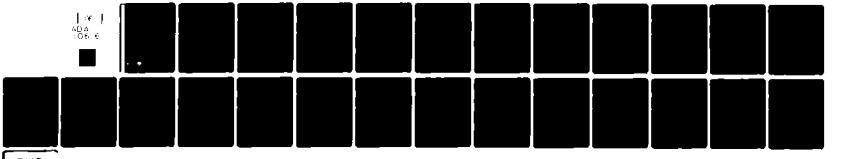

END
DATE FILMED
10-81
DTIC

ERC41018.3FR

Copy No. 10

PIEZOELECTRIC ZnS FILM ON SILICON

FINAL REPORT FOR THE PERIOD
November 1, 1979 through October 31, 1980

GENERAL ORDER NO. 41018

CONTRACT NO. F49620-79-C-0022

Prepared for

Air Force Office of Scientific Research
Bolling Air Force Base
Washington, D.C. 20332

Edward J. Staples
Principal Investigator

JUNE 1981

Approved for public release; distribution unlimited.

Rockwell International

UNCLASSIFIED

SECURITY CLASSIFICATION OF THIS PAGE (When Data Entered)

REPORT DOCUMENTATION PAGE

READ INSTRUCTIONS BEFORE COMPLETING FORM

1. REPORT NUMBER: AFOSR-TR-81-0682	2. GOVT ACCESSION NO.: AD-A105161
3. RECIPIENT'S CATALOG NUMBER	
4. TITLE (and Subtitle): PIEZOELECTRIC ZnS FILM ON SILICON	5. TYPE OF REPORT & PERIOD COVERED: FINAL REPORT 11/1/79 thru 10/31/80
	6. PERFORMING ORG. REPORT NUMBER: ERC41018.3FR
7. AUTHOR(s): EDWARD J. STAPLES	8. CONTRACT OR GRANT NUMBER(s): F49620-79-C-0022
9. PERFORMING ORGANIZATION NAME AND ADDRESS: MICROELECTRONICS RESEARCH AND DEVELOPMENT CENTER, ROCKWELL INTERNATIONAL CORPORATION, THOUSAND OAKS, CALIFORNIA 91360	10. PROGRAM ELEMENT, PROJECT, TASK AREA & WORK UNIT NUMBERS: 61102F 2306/B1
11. CONTROLLING OFFICE NAME AND ADDRESS: AIR FORCE OFFICE OF SCIENTIFIC RESEARCH, BOLLING AFB, WASHINGTON, D.C. 20332	12. REPORT DATE: June 1981
	13. NUMBER OF PAGES: 24
14. MONITORING AGENCY NAME & ADDRESS (if different from Controlling Office)	15. SECURITY CLASS. (of this report): UNCLASSIFIED
	15a. DECLASSIFICATION/DOWNGRADING SCHEDULE

16. DISTRIBUTION STATEMENT (of this Report)

APPROVED FOR PUBLIC RELEASE; DISTRIBUTION UNLIMITED

17. DISTRIBUTION STATEMENT (of the abstract entered in Block 20, if different from Report)

18. SUPPLEMENTARY NOTES

19. KEY WORDS (Continue on reverse side if necessary and identify by block number)

THIN FILM OF ZnS
PIEZOELECTRIC FILM
SURFACE ACOUSTIC WAVE DEVICE
SILICON

20. ABSTRACT (Continue on reverse side if necessary and identify by block number)

The objective of the present research investigation is to theoretically analyze the electromechanical coupling of piezoelectric zinc sulfide films on silicon substrates. During the past twelve months, considerable efforts have been made in analyzing the experimental results which were obtained in FY 1979. In order to accomplish this, a computer program was written to calculate surface-acoustic-wave electromechanical coupling constants for layered media. The calculation included four configurations of the excitation of surface acoustic waves in

DD FORM 1 JAN 73 1473 EDITION OF 1 NOV 65 IS OBSOLETE

UNCLASSIFIED

SECURITY CLASSIFICATION OF THIS PAGE (When Data Entered)

411391

different orientations of silicon using cubic and hexagonal ZnS films. The calculated results showed that the best acoustic coupling ~~(k^2)~~ for ZnS films is 10×10^{-4} which is an order of magnitude smaller than ZnO films on silicon. Also included in this report is the calculation of ZnO films on fused quartz and various orientation of silicon.

TABLE OF CONTENTS

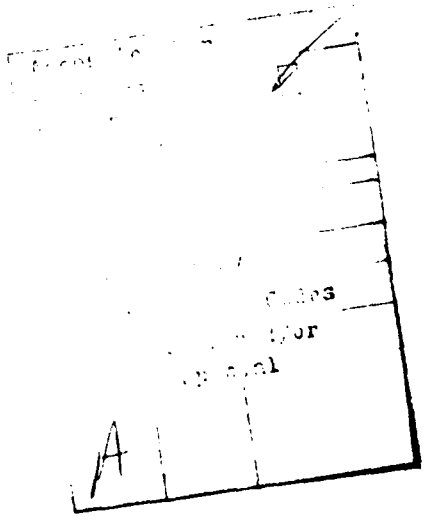

LIST OF TABLES

LIST OF FIGURES

1.0 SUMMARY

The objective of the present research investigation is to theoretically analyze the electromechanical coupling of piezoelectric zinc sulfide films on silicon substrates.

During the past twelve months, considerable efforts have been made in analyzing the experimental results which were obtained in FY 1979. In order to accomplish this, a computer program was written to calculate surface-acoustic-wave electromechanical coupling constants for layered media. The calculation included four configurations of the excitation of surface acoustic waves in different orientations of silicon using cubic and hexagonal ZnS films. The calculated results showed that the best acoustic coupling (k^2) for ZnS films is 10×10^{-4} which is an order of magnitude smaller than ZnO films on silicon. Also included in this report is the calculation of ZnO films on fused quartz and various orientation of silicon.

2.0 TECHNICAL BACKGROUND

In 1973, Inaba, Kajimura and Mikoshiba theoreticaly analyzed ZnS films on fused quartz[2] and showed that the SAW electromechanical coupling constant (k^2) was 7% which was three times larger than $LiNbO_3$. The same authors measured the coupling efficiency of ZnS films on boro-silicate glass at frequencies ranging from 70 to 90 MHz. The maximum film thickness tested was $0.1h/\lambda$ where λ is the SAW wavelength. The best conversion efficiency

for a 50 finger-pair transducer was 20 dB with electrodes at the interface and no ground plane.

In FY 1979, ZnS films were magnetron sputtered on 7059 glass as well as various orientations of silicon substrates at Rockwell. It was found that the best insertion loss obtained was 20 dB with 30 finger-pairs of interdigital transducers on the surface and a floating ground plane at the interface. This corresponds to a k^2 of 10×10^{-4}. Since the dispersion data of ZnS on glass or silicon were not available we decided to put the remaining effort into analyzing and calculating such layered media dispersion curves.

3.0 THEORETICAL RESULTS

3.1 Theoretical Analysis

The Japanese authors in reference 1 used the data published by Berlincourt et al[2] erroneously. The correct published value for e_{14}, the piezoelectric constant, is shown in Table 1.

Table 1
Elastic, Piezoelectric and Dielectric Constants of ZnS

Japanese Value	Rockwell Calculations
$C_{11} = 10.46 \times 10^{10}$ N/m^2	$C_{11} = 10.46 \times 10^{10}$ N/m^2
$C_{12} = 6.53$ "	$C_{12} = 6.53$ "
$C_{44} = 4.61$ "	$C_{44} = 4.6$ "
$e_{14} = 0.417$ (C/m^2)	$e_{14} = 0.14$ (C/m^2)
$\varepsilon_{11}/\varepsilon_0 = 8.32$	$\varepsilon_{11}/\varepsilon_0 = 8.32$
$\rho = 4083$ kg/m^3	$\rho = 4083$ kg/m^3

For cubic ZnS crystals, the non-vanishing matrix for elastic, piezoelectric and dielectric constants are given below

Elastic

$$C_{ij} = \begin{matrix} C_{11} & C_{12} & C_{12} & \cdot & \cdot & \cdot \\ C_{12} & C_{11} & C_{12} & \cdot & \cdot & \cdot \\ C_{12} & C_{12} & C_{11} & \cdot & \cdot & \cdot \\ \cdot & \cdot & \cdot & C_{44} & \cdot & \cdot \\ \cdot & \cdot & \cdot & \cdot & C_{44} & \cdot \\ \cdot & \cdot & \cdot & \cdot & \cdot & C_{44} \end{matrix}$$

Piezoelectric

$$e_{ij} = \begin{matrix} \cdot & \cdot & \cdot & e_{14} & \cdot & \cdot \\ \cdot & \cdot & \cdot & \cdot & e_{14} & \cdot \\ \cdot & \cdot & \cdot & \cdot & \cdot & e_{14} \end{matrix}$$

Dielectric

$$\varepsilon_{ij} = \begin{matrix} \varepsilon_{11} & \cdot & \cdot \\ \cdot & \varepsilon_{11} & \cdot \\ \cdot & \cdot & \varepsilon_{11} \end{matrix}$$

Since the sputtered ZnS films on glass are generally hexagonal in symmetry, a rotation of the matrix elements in the cubic system to (111)-plane will give the required elastic, piezoelectric and dielectric constants. The rotated non-vanishing matrix elements for (111) plane are given in Table 2.

Table 2

Rotated Elastic, Piezoelectric and Dielectric Constants
for (111) Plane of ZnS

Elastic

$$C_{ij} = \begin{matrix} C'_{11} & C'_{12} & C'_{13} & . & . & . \\ C'_{12} & C'_{11} & C'_{13} & . & . & . \\ C'_{13} & C'_{13} & C'_{33} & . & . & . \\ . & . & . & C'_{44} & . & . \\ . & . & . & . & C'_{44} & . \\ . & . & . & . & . & C'_{66} \end{matrix}$$

Where
$C'_{11} = 13.11 \times 10^{10}\ N/m^2$
$C'_{12} = 5.65$ "
$C'_{13} = 4.77$ "
$C'_{33} = 13.99$ "
$C'_{44} = 2.847$ "
$C'_{66} = 3.729$ "

Piezoelectric

$$e_{ij} = \begin{matrix} . & . & . & . & e'_{15} & . \\ . & . & . & e'_{15} & . & . \\ e'_{31} & e'_{31} & e'_{33} & . & . & . \end{matrix}$$

Where
$e'_{15} = -0.08\ C/m^2$
$e'_{31} = -0.081$ "
$e'_{33} = 0.162$ "

Dielectric

$$\varepsilon'_{ij} = \begin{matrix} \varepsilon_{11} & . & . \\ . & \varepsilon_{11} & . \\ . & . & \varepsilon_{111} \end{matrix}$$

Where $\varepsilon'_{11}/\varepsilon_0 = 8.32$

Consider a surface wave propagating along the x-axis of the layered media shown in Fig. 1 with x_3 axis normal to the surface. The stress equation is given as:

$$\frac{\partial T_{ij}}{\partial x_j} = \rho \frac{\partial^2 U_i}{\partial t^2} \tag{1}$$

where T_{ij} is the stress, U_j the mechanical displacement and ρ the density. The electric displacement D_i for an insulating material such as ZnS,

$$\frac{\partial D_i}{\partial x_i} = 0 \tag{2}$$

For piezoelectric material, the equations of motion are given as:

$$T_{ij} = C^E_{ijk\ell}\, S_{k\ell} - e_{kij}\, E_k \tag{3}$$

$$D_i = e_{ik\ell}\, S_{k\ell} + \varepsilon^S_{ik}\, E_k \tag{4}$$

Where $S_{kl} = 1/2(\partial U_k/\partial x_\ell + \partial U_\ell/\partial x_k)$ are components of strain, $E_k = \partial\phi/\partial x_k$ the electric field, $C_{ijk\ell}$ the elastic constants at constant electric field, e_{kij} the piezoelectric constants and ε^S_{ik} the dielectric permittivity tensor at constant strain.

Substituting Eqs. (1) and (2) into (3) and (4) to give

$$\frac{\partial Tij}{\partial x_j} = \frac{1}{2}\; C^E_{ijk\ell}\, \frac{\partial}{\partial k_j} \left(\frac{\partial U_k}{\partial k_\ell} + \frac{\partial U_\ell}{\partial x_k}\right) + e_{kij}\, \frac{\partial^2 \phi}{\partial x_j \partial x_k} = \rho \frac{\partial^2 U_i}{\partial t^2} \tag{5}$$

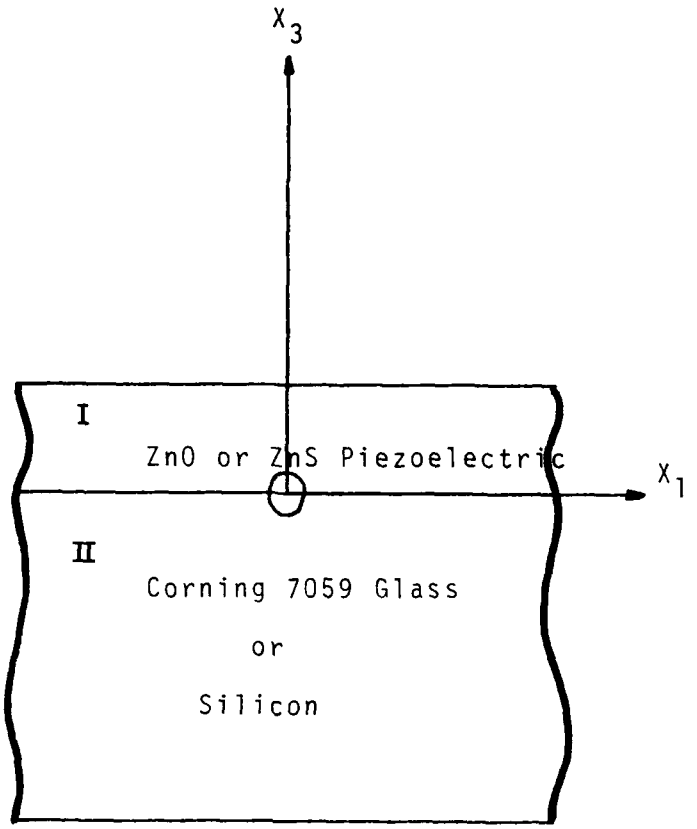

Fig. 1 A layer of ZnO or ZnS piezoelectric films on glass or silicon substrates.

$$\frac{1}{2} e_{ik\ell} \frac{\partial}{\partial x_i} \left(\frac{\partial U_k}{\partial x_\ell} + \frac{\partial U_\ell}{\partial x_k}\right) - \varepsilon^S_{ik} \frac{\partial^2 \phi}{\partial x_i \partial x_k} = 0 \qquad (6)$$

$$i, j, k, \ell = 1, 2, 3$$

Assuming a particle displacement of the form

$$U_j = \alpha_j e^{ikbx_3} e^{ik(x_1 - vt)} \qquad (7)$$

where α_j are unit vectors along x_j respectively; wave member $k = 2\pi/\lambda$, b the decay constant with depth and v the phase velocity; and the electric potential as

$$\phi = \alpha_4 e^{ikbx_3} e^{ik(x_1 - vt)} \qquad (8)$$

Substituting Eqs. (7) and (8) into (5) and (6) gives:

$$\begin{bmatrix} \Gamma_{11} - \rho V^2 & \Gamma_{12} & \Gamma_{13} & \Gamma_{14} \\ \Gamma_{12} & \Gamma_{22} - \rho V^2 & \Gamma_{23} & \Gamma_{24} \\ \Gamma_{13} & \Gamma_{23} & \Gamma_{33} - \rho V^2 & \Gamma_{34} \\ \Gamma_{14} & \Gamma_{24} & \Gamma_{34} & \Gamma_{44} \end{bmatrix} \cdot \begin{bmatrix} \alpha_1 \\ \alpha_2 \\ \alpha_3 \\ \alpha_4 \end{bmatrix} = 0 \qquad (9)$$

where

$$\Gamma_{11} = C_{55}\, b^2 + 2C_{15}\, b + C_{11}$$
$$\Gamma_{22} = C_{44}\, b^2 + 2C_{46}\, b + C_{66}$$
$$\Gamma_{33} = C_{33}\, b^2 + 2C_{35}\, b + C_{55}$$
$$\Gamma_{12} = C_{45}\, b^2 + (C_{14} + C_{56})\, b + C_{16}$$
$$\Gamma_{13} = C_{35}\, b^2 + (C_{13} + C_{55})\, b + C_{15}$$
$$\Gamma_{23} = C_{34}\, b^2 + (C_{36} + C_{45})\, b + C_{56}$$
$$\Gamma_{14} = e_{35}\, b^2 + (e_{15} + e_{31})\, b + e_{11}$$
$$\Gamma_{24} = e_{34}\, b^2 + (e_{14} + e_{36})\, b + e_{16}$$
$$\Gamma_{34} = e_{33}\, b^2 + (e_{13} + e_{35})\, b + e_{15}$$

with the electric term

$$\Gamma_{44} = -(\varepsilon_{33}\, b^2 + 2\,\varepsilon_{13}\, b + \varepsilon_{11})$$

The secular Eq. (9) is applied to the layer and substrate regions and the matrix of coefficients is reduced to a polynomial in b. In the completely general case the polynomial is of 8th order and 8 complex roots, b_j are solved for. For the substrate, only those roots which cause decay to zero with decreasing x_3 are retained. This results in 12 solutions to the equation of motion (3).

The total solution to the layered problem is taken as a sum of the 12 partial solutions,

$$\Phi_j = \sum_{L,S} C_n\, \alpha_j^{(n)}\, e^{ikb_n x_3}\, e^{ik(x_1 - vt)} \qquad (10)$$

$$\bar{\phi} = \sum_{L,S} C_n \alpha_4^{(n)} e^{ikb_n x_3} e^{ik(x_1 - vt)} \qquad n = 1,2,3$$

where $\sum_{L,S}$ indicates summation over root numbers, n, for the layer (L) and substrate (S).

The general boundary conditions are:

a) Mechanical Transverse

1. Continuity of transverse displacement at the interface

$$U_s^S = \hat{U}_2^{\ell} \qquad \text{at } x_3 = 0$$

2. Continuity of transverse shear stress at interface

$$T_{32}^S = \hat{T}_{32}^{\ell} \qquad \text{at } x_3 = 0$$

3. Vanishing of transverse shear stress at the free surface

$$\hat{T}_{32}^{\ell} = 0 \qquad \text{at } x_3 = h$$

b. Electrical

4. Continuity of the normal component of electrical displacement at interface

$$D_3^S = \hat{D}_3^{\ell} \qquad \text{at } x_3 = 0$$

5. Continuity of potential at interface

$$\phi^s = \hat{\phi}^\ell \qquad \text{at } x_3 = 0$$

6. Continuity of normal component of electrical displacement at free surface

$$\hat{D}_3^\ell = k\,\varepsilon_o\,\hat{\phi}^\ell \quad \text{at } x_3 = h \qquad \left(\text{for } \hat{D}_3^\ell = -\,\varepsilon_o \frac{\partial \phi^\ell}{\partial x_3} \text{ when } x_3 \to \infty\right)$$

c. Mechanical Sagittal

7. Continuity of longitudinal particle displacement at interface

$$U_1^s = \hat{U}_1^\ell \qquad \text{at } x_3 = 0$$

8. Continuity of vertical particle displacement at interface

$$U_3^s = \hat{U}_3^\ell \qquad \text{at } x_3 = 0$$

9. Continuity of sagittal shear stress at interface

$$T_{31}^s = \hat{T}_{31}^\ell \qquad \text{at } x_3 = 0$$

10. Continuity of vertical compressional stress at interface

$$T_{33}^s = \hat{T}_{33}^\ell \qquad \text{at } x_3 = 0$$

11. Vanishing of sagittal shear stress at free surface

$$\hat{T}^{\ell}_{31} = 0 \qquad \text{at } x_3 = h$$

12. Vanishing of vertical compressional stress at free surface

$$\hat{T}^{\ell}_{33} = 0 \qquad \text{at } x_3 = h$$

If the surface or interface is conducting then the conditions on displacements D_3 are changed to reflect a zero potential at the appropriate value of x_3. Thus the above 12 boundary conditions provide 12 equations in the 12 unknowns, C_n. The matrix elements of the general boundary condition determinant are shown in Table 3.

In order to obtain non-trivial solutions to this set of homogeneous equations, a 12 x 12 determinant, successive values of v are chosen until the boundary condition determinant is equal to zero.

A computer program based on the above analysis was developed to calculate the dispersion characteristics and electromechanical coupling constants of ZnO and ZnS transducers using the piezoelectric data of Berlincourt et al.[2]

3.2 Zinc Oxide Films on Fused Quartz and Silicon

As a test of the computer program and for comparison of performance with ZnS films, ZnO on fused quartz and (111) silicon substrates was analyzed.

Table 3

Boundary-condition Determinant for General Case

Row	"Substrate" columns m (four values)	"Layer" Columns n (eight values)
1.	α_2^m	$-\alpha_2^n$
2.	$(c_{32i1} + c_{32i3}b^m)\alpha_i^m + (e_{132} + e_{332}b^m)\alpha_4^m$	$-(\hat{c}_{32i1} + \hat{c}_{32i3}b^n)\alpha_i^n - (\hat{e}_{132} + \hat{e}_{332}b^n)\alpha_4^n$
3.	0	$[\hat{c}_{32i1} + \hat{c}_{32i3}b^n)\alpha_i^n + (\hat{e}_{132} + \hat{e}_{332}b^n)\alpha_4^n]\exp(ikb^nh)$
4.	$(e_{3i1} + e_{3i3}b^m)\alpha_i^m - (e_{31} + 3_{33}b^m)\alpha_4^m$	$-(\hat{e}_{3i1} + \hat{e}_{3i3}b^n)\alpha_i^n + (\hat{e}_{31} + \hat{e}_{33}b^n)\alpha_4^n$
5.	α_4^m	$-\alpha_4^n$
6.	0	$[-(\hat{e}_{3i1} + e_{3i3}b^n)\alpha_i^n + (\hat{\epsilon}_{31} + \hat{\epsilon}_{33}b^n - i\epsilon_0)\alpha_4^n]\exp(ikb^nh)$
7.	α_1^m	$-\alpha_1^n$
8.	α_3^m	$-\alpha_3^n$
9.	$(c_{31i1} + c_{33i3}b^m)\alpha_i^m + (e_{131} + e_{331}b^m)\alpha_4^m$	$-(\hat{c}_{31i1} + \hat{c}_{31i3}b^n)\alpha_i^n - (\hat{e}_{i31} + \hat{e}_{331}b^n)\alpha_4^n$
10.	$(c_{33i1} + c_{33i3}b^m)\alpha_i^m + (e_{133}b^m)\alpha_4^m$	$-(\hat{c}_{33i1} + \hat{c}_{33i3}b^n)\alpha_i^n - (\hat{e}_{133} + \hat{e}_{333}b^n)\alpha_4^n$
11.	0	$[(\hat{c}_{31i1} + \hat{c}_{31i3}b^n)\alpha_i^n + (\hat{e}_{131} + \hat{e}_{331}b^n)\alpha_4^n]\exp(ikb^nh)$
12.	0	$[(\hat{c}_{33i1} + \hat{c}_{33i3}b^n)\alpha_i^n + (\hat{e}_{133} + \hat{e}_{333}b^n)\alpha_4]\exp(ikb^nh)$

The results for ZnO on fused quartz are shown in Fig. 2. Figure 2a shows the velocity dispersion as a function of layer thickness normalized to wavelength over the range 0.001 to 5. The normalized velocity change ($\Delta V/V$) corresponding to a transducer (electrodes on top, ground plane at interface) shown in Fig. 2b. These calculations were checked against previously published results of Kino and Wagers [3] for comparison. The coupling peak at 5% is approximately 5×10^{-3}.

A similar calculation was then made for ZnO on (111), <110> silicon and the results are shown in Fig. 3. The maximum coupling peak again was at 5% however somewhat reduced to 3×10^{-3}.

3.3 ZnS Films on Fused Quartz and Silicon

After determining the correctness of our ZnO calculations, the analysis of ZnS films was performed. The first material analyzed was ZnS on fused quartz. Surface wave velocity and coupling were computed for all four possible transducer configurations as shown in Fig. 4. The peak in coupling at 5% was much less than the previous ZnO result, i.e., 1×10^{-4}. This is not equal to $LiNbO_3$ and more than an order of magnitude less than ZnO on fused quartz.

ZnS films on (001) propagation along <100> and (111), <1$\bar{1}$0> silicon were also analyzed. The results are shown in Fig. 5 and 6. On (001) silicon the coupling at 5% was 1×10^{-4} and on (111) the coupling was 0.5×10^{-4}.

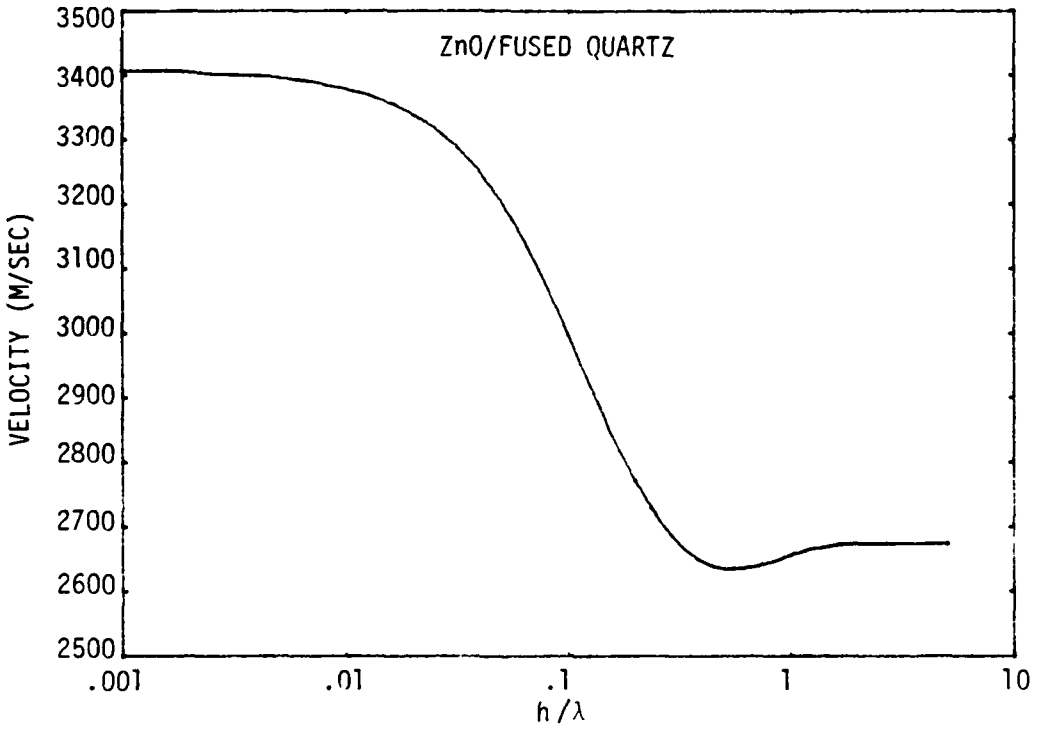

(a)

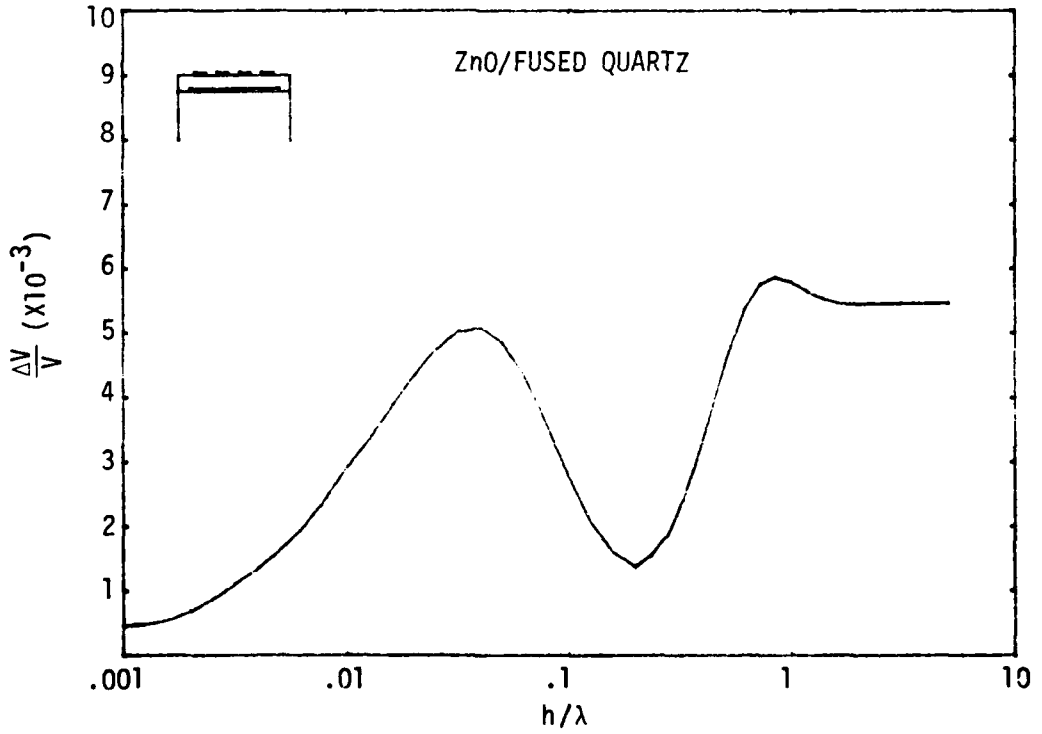

(b)

Fig. 2 ZnO film on fused quartz; a) Phase velocity and b) electromechanical coupling constant $k^2(2\ \Delta V/V)$ as a function of h/λ.

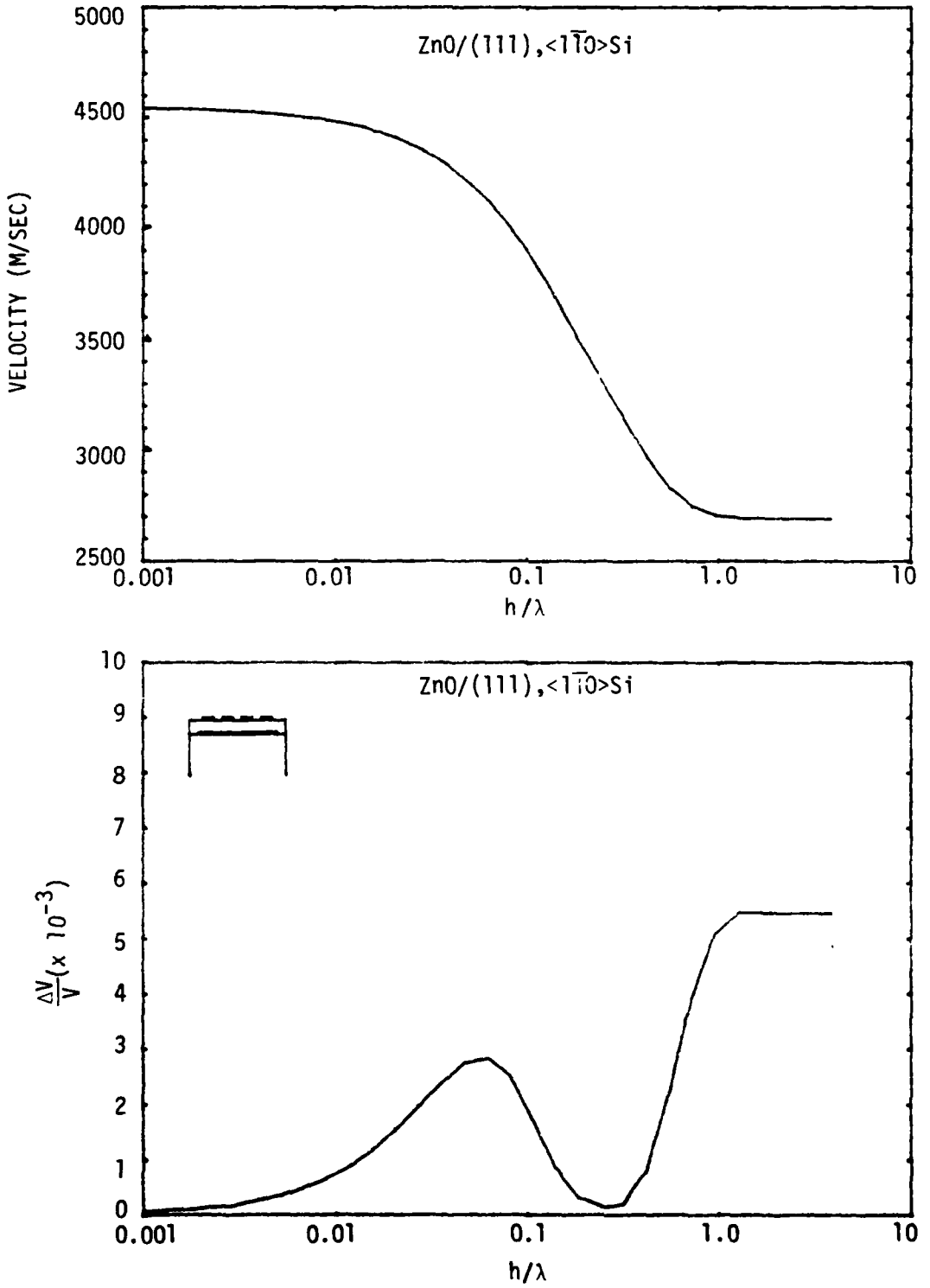

Fig. 3 ZnO film on (111)-plane of Si with propagation vector along <1$\bar{1}$0> direction; a) phase velocity and b) electromechanical coupling $k^2(2\ \Delta V/V)$ as a function of h/λ.

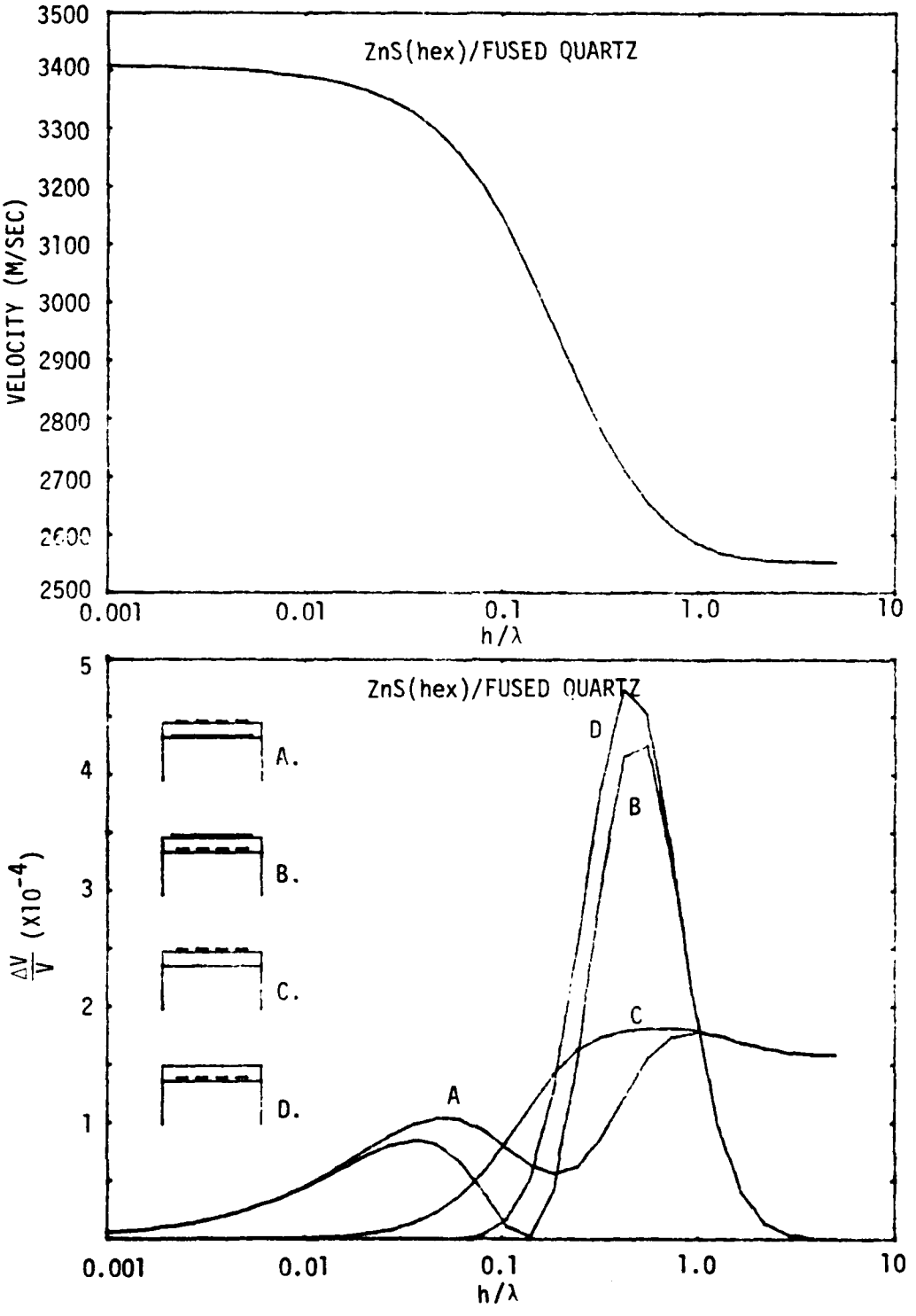

Fig. 4 ZnS film on fused quartz; a) phase velocity and b) electromechanical coupling of excitation as a function of h/λ.

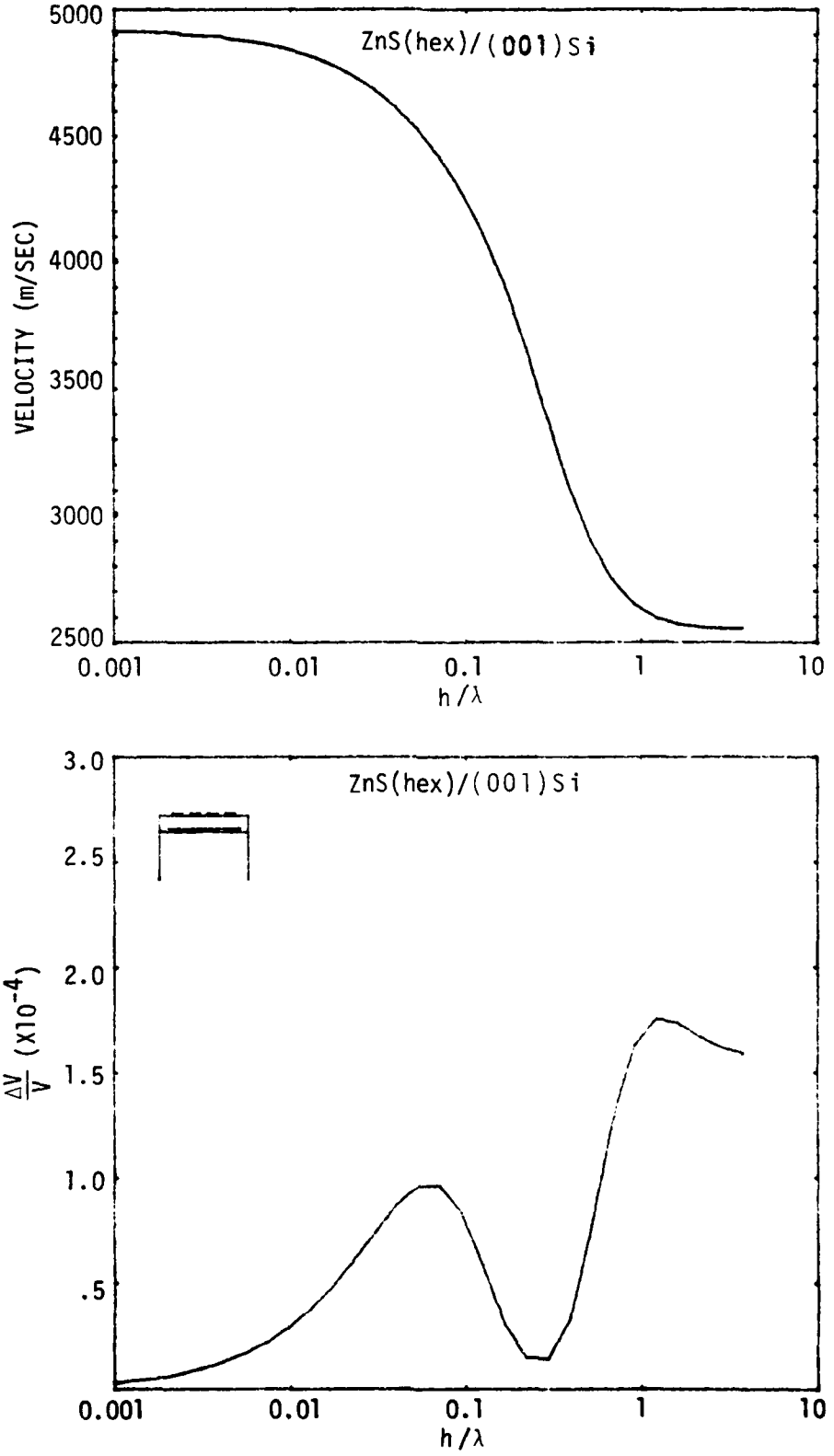

Fig. 5 ZnS film on (001) plane of Si with propagation vector along <100> direction; a) phase velocity and b) electromechanical coupling constant as a function of h/λ.

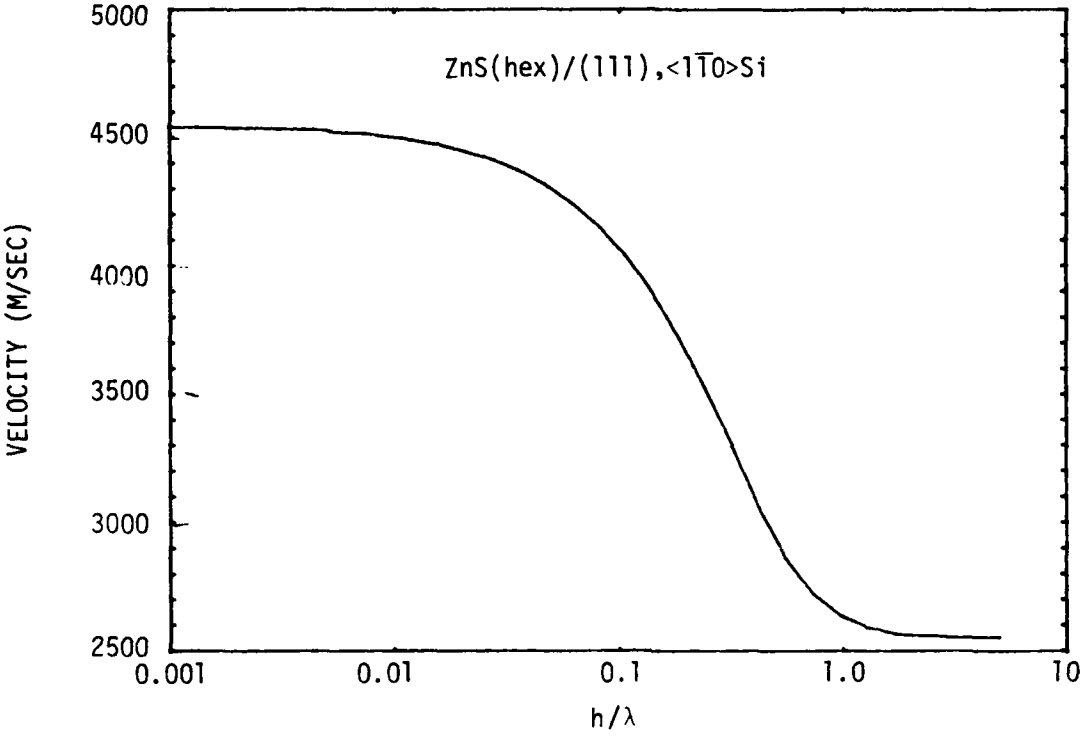

(a)

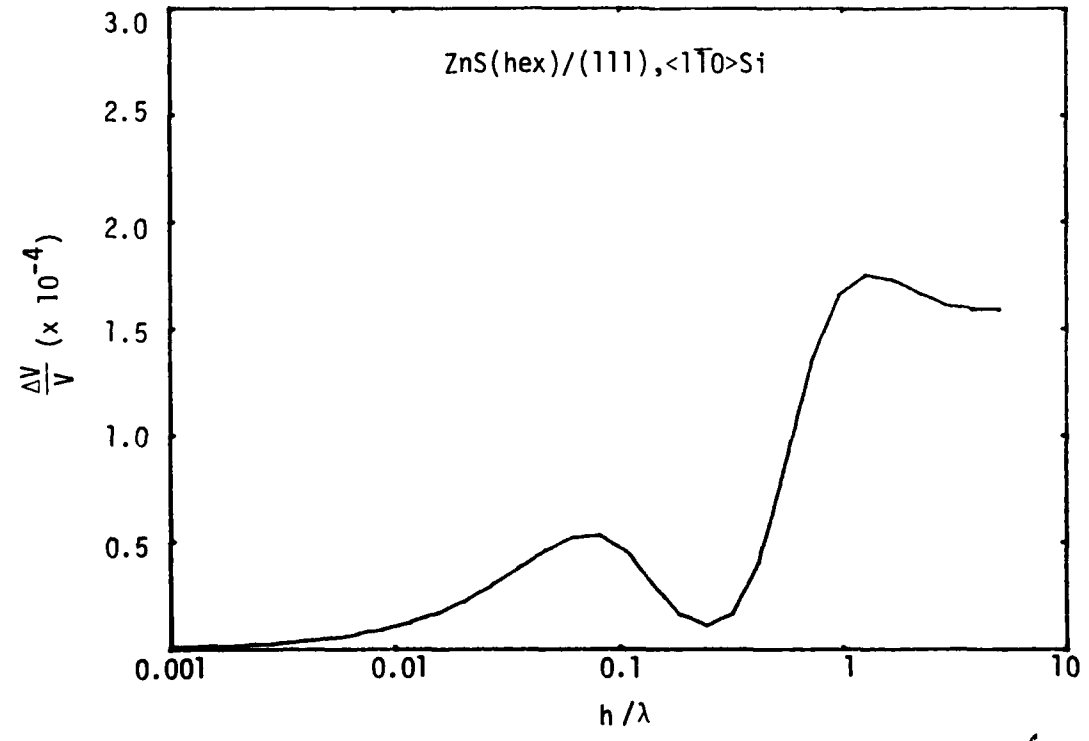

(b)

Fig. 6 ZnS film on (111)-plane of Si, propagation vector along <1$\bar{1}$0> direction; a) phase velocity and b) electromechanical coupling constant (2 $\Delta V/V$) as a function of h/λ.

4.0 CONCLUSIONS

Theoretical calculations were performed on ZnO and ZnS films on silicon and fused quartz substrates. ZnO typically showed a peak in coupling of 5×10^{-3} at 5% thickness normalized to wavelength. ZnS films were found to have considerably less, typically 1×10^{-4} at the same film thickness. This result directly conflicts with previously published calculations [1]. However, comparing the ZnO and ZnS (hexagonal) piezoelectric constants in Table 4, the result is expected. This is substantiated by our experimental measurements on ZnS film coupling.

Table 4

Piezoelectric Constants of ZnO and Rotated ZnS

ZnO	ZnS
$e_{33} = 1.321$	$e_{33} = 0.162$
$e_{31} = 0.573$	$e_{31} = -0.081$
$e_{15} = -0.480$	$e_{15} = -0.0818$

5.0 REFERENCES

1. R. Inaba, K. Kajimura, and N. Mikoshiba, "Thickness Dependence of Conversion Efficiency of ZnS Film Transducers for Elastic Surface Waves," J. Appl. Phys. Vol. 44, No. 6, p. 2495-2503, June 1973.
2. D. Berlincourt, H. Jaffe, and L. Shiozawa, "Electro-elastic Properties of the Sulfides and Tellurides of Zinc and Cadmium," Physical Review, Vol. 129, No. 3, p. 1009-1017, Feb, 1963.
3. G. Kino and R. Wagers, "Theory of Interdigital Couplers on Non-piezoelectric Substrates," J. Appl. Phys., Vol. 44, No. 4, April 1973, p. 1480-1488.

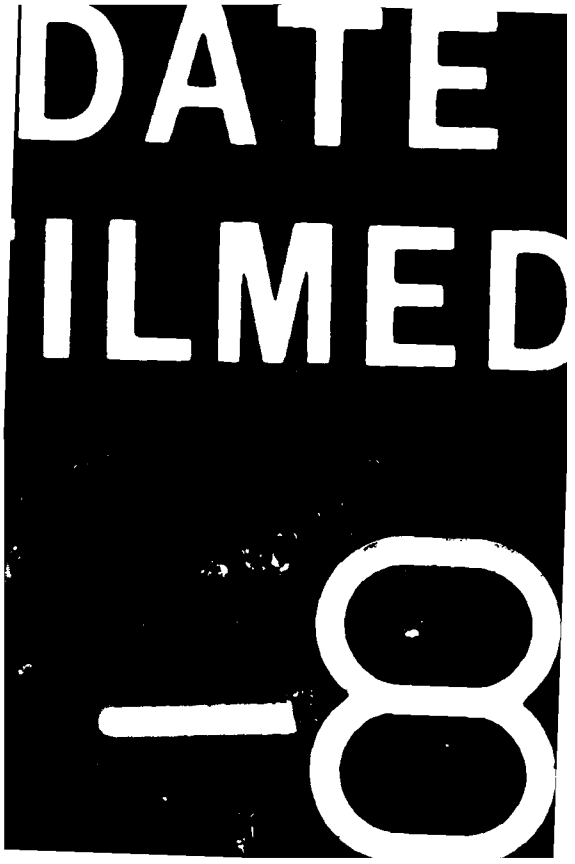
DATE
ILMED
8